Near surface turbulence and its relationship to air–water gas transfer rates

Damon Turney[1] and Sanjoy Banerjee[2]

[1] *Energy Science and Technology Department, Brookhaven National Laboratory, Upton, NY USA Email: dturney@bnl.gov*

[2] *Department of Chemical Engineering, The City College, City University of New York, New York, NY USA E-mail: banerjee@che.ccny.cuny.edu*

Abstract. Values for the air-water gas transfer coefficient k depend on the interplay between near surface flow and chemical concentration fields. Since direct simulations are not yet possible the prediction of k must proceed through simplified models of the governing equations or by use of empirical parameterizations. Several of the leading models are not yet tested because the necessary measurements of near surface flow are difficult. Here we use new techniques called Interfacial Particle Imaging Velocimetry (IPIV) and three-dimensional IPIV (3D-IPIV) for measuring near surface flow fields and interfacial morphology simultaneously, applied to open channel flow and wind wave conditions. We test the McCready *et al*. (1986) and the Banerjee (1990) surface divergence theories in open channel flow, finding that both agree well with measurements. The McCready theory is also tested in wind wave flows, but the inception of capillary waves is found to cause disagreement between the theory and measurements. Issues of surface renewal are found to play an important role. Based on these observations, a new model incorporating both surface renewal and surface divergence is proposed, which finds good agreement in all of our experimental conditions.

Key Words: Air-Water Gas Transfer, Interface, Turbulence, Wind Waves, PIV

1. Introduction

Gas and volatile chemicals budgets in air-water systems are important in a wide variety of settings, e.g., for industrial equipment such as boilers, condensers, absorbers, and also for environmental purposes such as budgeting CO_2, or understanding the fate of mercury emissions from power plants. Unfortunately these budgets are difficult to develop because the air-water interfacial transfers are poorly predicted. Uncertainty in predictions of the transfer rate is typically greater than a factor of 2. The central problem lies in the interplay between near surface fluid motions and chemical concentrations, both of which are difficult to measure or model (Hunt *et al*. 2010; Komori *et al*. 1993).

Table 1 A list of the more commonly used models of air-water gas transfer. For these equations D is the chemical diffusivity, δ is the Lewis-Whitman thickness of the concentration boundary layer, τ is the length of time between surface renewal events where an overbar denotes a spatio temporal average, L is the turbulent integral length scale, u' is the turbulence intensity far from the interface, Sc is the Schmidt number Re_t is the turbulent Reynolds number, C is a coefficient, and β' is the rms of surface divergence values at the interface.

Authors	Name	Prediction of k
(Lewis and Whitman 1924)	film	$\bar{k}=D/\delta$
(Higbie 1935)	penetration	$\bar{k}=\sqrt{D/(\pi\tau)}$
(Danckwerts 1951)	surface renewal	$\bar{k}=\sqrt{D/\bar{\tau}}$
(Fortescue and Pearson 1967)	large eddy	$\bar{k}=\sqrt{D/\bar{\tau}}$ with $\bar{\tau}\approx L/u'$, giving $\bar{k}=Cu'Sc^{-1/2}\mathrm{Re}_t^{-1/2}$
(Banerjee, et al. 1968)	small eddy	$\bar{k}=\sqrt{D/\bar{\tau}}$ with $\bar{\tau}\approx\sqrt{\nu/\varepsilon}$, giving $\bar{k}=Cu'Sc^{-1/2}\mathrm{Re}_t^{-1/4}$
(McCready et al. 1986)	surface divergence	$\bar{k}=C\sqrt{D\beta'}$
(Banerjee 1990)	surface divergence based on Hunt and Graham (1978)	$\bar{k}=Cu'Sc^{-1/2}\mathrm{Re}_t^{-1/2}\,[0.3(2.83\mathrm{Re}_t^{3/4}-2.14\mathrm{Re}_t^{2/3})]^{1/4}$

In practice, predictions of the chemical flux across the interface F for sparingly soluble gases are based on the resistance to mass transfer being primarily on the liquid side giving

$$F=k[c_{ba}-Sc_{bw}] \tag{1}$$

where c_{ba} is the concentration in the bulk air, S is the solubility in water, c_{bw} is the concentration in the bulk water, and k is a constant called the gas transfer coefficient. For highly soluble gases, an equivalent equation would apply on the airside. Equation (1) arises from the advection-diffusion and Navier-Stokes equations, by noting that both are linear with respect to concentration, and therefore the flux F must be proportional to the concentration boundary conditions c_{ba} and c_{bw}. The value of the transfer coefficient k depends on the interaction between near surface velocity, as governed by the Navier-Stokes equations, and the concentration field, as governed by the advection-diffusion equation. The equations are usually impractical to solve by computation, therefore k must be estimated by simplifications of the governing equations, often called models or theories, or by use of empirical parameterizations. This paper focuses on testing the validity of the models, the most commonly used of which are listed in Table 1.

Unfortunately most of these models remain untested because measurement of the parameters τ, β', L, u', or ε is difficult near the air-water interface. To make the measurements one must observe the motion of water within ~1 millimeter of the interface, a difficult task, which is made more difficult when wind waves cause the interface to rapidly deform and move. Computer simulations have provided estimates of these parameters for simple flow conditions at lower turbulent Reynolds numbers, but simulation is too costly for high Reynolds number cases. In this paper we report tests of several of the models listed in Table 1, using both computer simulation and laboratory measurements.

2. Experiments

Computational studies were performed to simulate the Navier-Stokes equations. Details are given by Lombardi *et al*. (1996) and Fulgosi *et al*. (2003). The simulations were typically performed with shear Reynolds numbers (based on interfacial shear stress) of a few hundred both the air and water phases. Turbulence generation was only at the interface with the confining boundaries for the stratified two-phase flows being slip walls. The simulations were run out in time till the turbulence and interfacial wave structure were fully developed. The numerical technique used could not handle wave breaking so interfacial shear velocity based on liquid side density was typically kept below 0. 1 m/s. As discussed later much could be learned from theses simulations for gas transfer at low wind velocities.

All experimental measurements were conducted in a laboratory at the University of California, Santa Barbara, in a horizontal channel of length 12.0 m, width 0.70 m, and height 0.30 m through which a stratified air-water flow could be established. The upstream end of the channel was equipped with flow straighteners, a wave suppressor, dissolved oxygen stripping equipment, and a large fan for generating wind inside the channel. The downstream end of the channel held dissolved oxygen probes, wind sensors, wave height gauges, and high-speed cameras that could view the water flow through glass and plexiglass sidewalls. The cameras were mounted on a belt-driven track that moved them downstream at the average interfacial velocity. The dissolved oxygen equipment allowed determination of the air-water gas transfer coefficient $\overline{k}$ spatially averaged over the final two meters of the channel. The overbar denotes a spatial and temporal average. For flow conditions without wind, i.e., open channel flow, five water depths were investigated, ranging between 5 and 13 cm, and for each depth four water velocities were investigated. The left side of Table 2 gives a full listing of the open channel flow conditions. The windy flow conditions included thirteen wind velocities, listed on the right of Table 2. Further description of our equipment and methods is given in a dissertation by Turney (2009a).

To measure near-surface water motions quantitatively, we developed new

Table 2 Conditions for the experiments. On the left are the flow conditions for open channel flows without wind. On the right are conditions for the flows with wind forcing.

Id.	Water Depth h (m)	Surface Velocity $\bar{u}_s$ (m/s)	Surface Reynolds Number Re_s $\frac{\bar{u}_s h}{\upsilon}$	Width to Depth Ratio w_c/h	Distance to Measurement Section d/h
R1	0.050	0.023	1150	14.0	160
R2	0.050	0.030	1500	14.0	160
R3	0.050	0.100	5000	14.0	160
R4	0.050	0.240	12000	14.0	160
R5	0.050	0.600	30000	14.0	160
R6	0.055	0.545	30000	12.7	145
R7	0.070	0.071	5000	10.0	114
R8	0.070	0.171	12000	10.0	114
R9	0.070	0.429	30000	10.0	114
R10	0.090	0.056	5000	7.7	88
R11	0.090	0.133	12000	7.7	88
R12	0.090	0.333	30000	7.7	88
R13	0.100	0.107	10700	7.0	80
R14	0.100	0.058	5800	7.0	80
R15	0.130	0.038	5000	5.4	62
R16	0.130	0.092	12000	5.4	62
R17	0.130	0.231	30000	5.4	62

Id.	Water Depth h (m)	Air-Water Friction Velocity u_{*a} (m/s)	Ten Meter Height Windspeed U_{10} (m/s)
W1	0.05	0.03	1.1
W2	0.05	0.03	1.1
W3	0.05	0.04	1.5
W4	0.05	0.07	2.4
W5	0.05	0.09	3.0
W6	0.10	0.10	3.1
W7	0.10	0.13	4.1
W8	0.10	0.16	5.0
W9	0.10	0.20	6.0
W10	0.10	0.24	7.1
W11	0.10	0.24	7.0
W12	0.10	0.28	8.0
W13	0.10	0.32	8.9

particle imaging velocimetry techniques that allowed measurement of water velocity within one millimeter of the interface and simultaneous measurement of the morphology of the interface. Figure 1 shows a schematic of these techniques, wherein the water is dyed black and seeded with fluorescent-red microspheres stimulated by a blue overhead light. The microspheres are only visible within one millimeter of the air-water interface, even when the interface is wavy. Placing a red filter in front of the cameras eliminates reflections of blue light from the air-water interface. The velocity of water at the interface may then be determined by standard digital velocimetry methods. This new technique is termed Interfacial Particle Imaging Velocimetry (IPIV).

The three-dimensional shape of the interface may also be measured if two cameras view the interface from different angles, giving simultaneous morphology and velocimetry results, termed Three-Dimensional IPIV (3D-IPIV). Details of the methods are found in Turney *et al.* (2009b).

The 3D-IPIV technique was used to characterize the near-surface motions for all the wind-forced conditions listed in Table 2, and the more simple IPIV

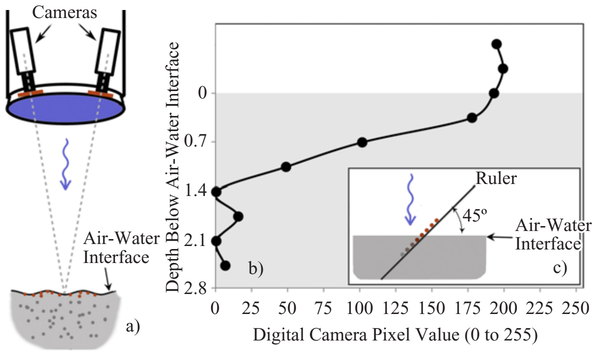

Figure 1 A schematic of the 3D-IPIV technique, showing a) the two high-speed cameras set up for three-dimensional measurements, b) our recordings of the visibility of microspheres under the water surface, and c) our method used for measuring the visibility of microspheres under the water surface.

technique was used for each of the open channel flow conditions in Table 2. For the open channel flows the turbulent motions in the bulk water, ~5 cm below the interface, were also measured by typical side-view PIV techniques. Turbulence length scales and intensities were calculated for all velocity recordings. For all flows, the air-water transfer coefficient is also measured.

3. Results and discussion

3.1 Computational Results

The direct numerical simulations of air-water streams where shear is only at the interface indicate that mass transfer at interfacial shears low enough that waves do not break is governed by liquid-side sweeps that bring bulk liquid to the interface. In the absence of breaking the near-interface turbulence structure is quite similar to that near solid boundaries except that interface parallel fluctuations on the liquid side are not damped. Streaky structures and ejection/sweep cycles are seen as discussed extensively by Lam and Banerjee (1992), Lombandi *et al.* (1996), De Angelis *et al.* (1998), and Fulgosi *et al.* (2003). In any case it is found that a surface renewal theory based on interfacial sweeps as constituting surface renewal events gives rise to parameterization based on sweep frequency in liquid side controlled mass transfer as

$$\frac{kSc^{1/2}}{u^*} \sim 0.1 \text{ to } 0.15$$

where u^* and Sc are the liquid side Schmidt number and shear velocity

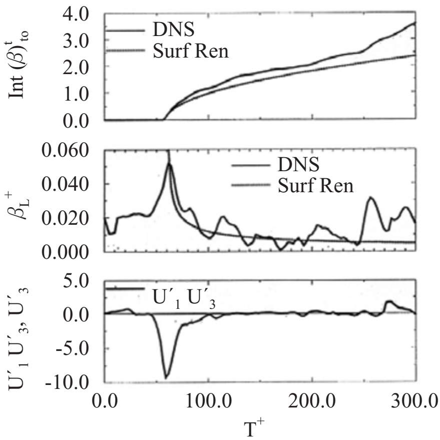

Figure 2 Simulation results of mass transfer arising from arrival of a sweep at the interface compared with predictions of surface renewal theory. (β_L_is the liquid side mass transfer coefficient, u''_1, u'_3 are the streamwise and interface-normal velocity flunctuations).

respectively. The reason why this parameteorization works is illustrated in Figure 2 which shows in the bottom panel the arrival of a sweep (with u_3' large and negative, i.e. high speed fluid coming towards the interface). The mass transfer rate from the simulation is seen to peak when this happens for a surface renewal event in the second panel. The first panel compares the cumulative mass transfer rate following the renewal event from the simulation with the calculations of surface renewal theory.

3.2 Experimental Results for Open Channel Flows

Figure 3 shows the comparison between the McCready *et al.* (1986) surface divergence prediction, for the average mass transfer coefficient $\overline{k}=C\sqrt{D\beta'}$, as calculated from our measurements of β', the rms surface divergence of the velocity fluctuations and our direct measurements of $\overline{k}$ for open channel flows. Good agreement is seen between the theory and the data, which is noteworthy because it is the first test of the surface divergence theory in open channel flow with direct measurements of β'.

Figure 4 shows a comparison between the Banerjee (1990) surface divergence theory and our direct measurements of $\overline{k}$, with a coefficient of 0.2. The solid lines and solid squares are direct measurements of $\overline{k}$ from our laboratory. The dashed lines and open squares are predictions from the theory, i.e., the last equation in Table 1. Reasonable agreement is seen between the theory and empirical

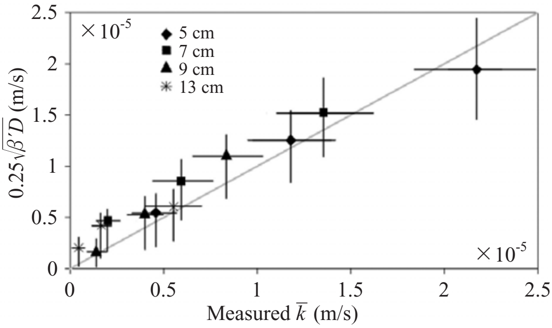

Figure 3. A comparison of the McCready *et al*. (1986) surface divergence theory against direct measurements of the interfacial transfer rate, for open channel flows with no wind. The lines extending from the data points give the measurement error.

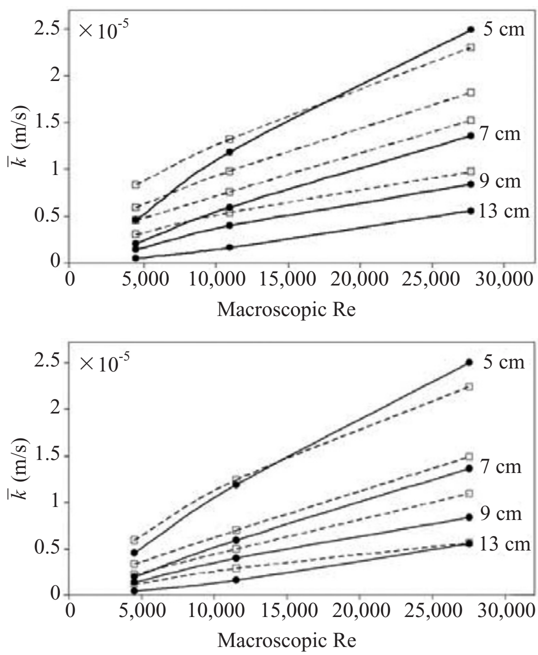

Figure 4 A test of the Banerjee (1990) surface divergence theory is shown. The solid circles and solid lines correspond to our empirical measurements of $\overline{k}$. The open squares and dashed lines correspond to the predictions from the Banerjee theory based on our empirical measurements of L and u'. The top plot is the straight calculation of the Banerjee theory. The bottom side plot uses u_i' instead of u' in the calculations.

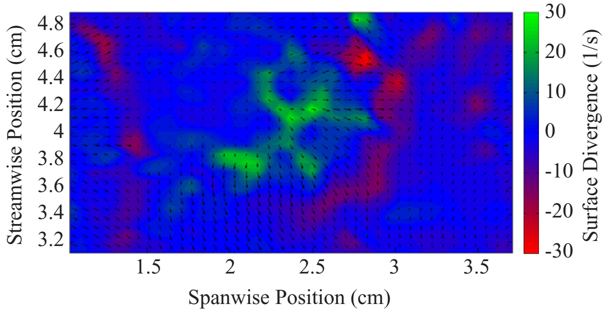

Figure 5 A zoomed in portion of surface divergence measurements is shown by the color plot. Velocity vectors, gathered by our IPIV methods, are overlain as black arrows. The surface divergence values are calculated from the velocity vectors.

measurements, which is remarkable given that the theory is based on turbulence values measured far from the interface. On the bottom in Figure 4 is the same comparison but the interfacial turbulence intensity u_i' is used in the calculation of the Banerjee (1996) surface divergence theory instead of the bulk turbulence intensity u', and better agreement is seen. The better agreement with u_i' values arises because small amounts of surfactants were seen present on the air-water interface, which damped the interfacial motions. Before each experiment we vacuumed the interface with a surface skimmer for at least 30 minutes, but it is our opinion that the interface can never by made fully clean unless highly purified water and an extremely clean laboratory is used.

Figure 5 shows a zoomed in portion of our surface divergence measurements in open channel flows. Vectors of surface velocity are plotted over the top as black arrows. It can be seen that the surface divergence patterns are of smaller spatial scale than the upwellings. Further, much of the interface has relatively low surface divergence. We will discuss later that regions of surface divergence have to persist for a minimum lifetime, which depends on their intensity, before they are effective in mass transfer. This leads to an approach which requires concepts from the surface divergence and surface renewal theories to be combined.

3.3 Experimental Results for Wind Wave Flows

The 3D-IPIV method gives greatly improved measurements of surface divegence at the air-water interface under wind sheared conditions. The average surface divergence value β' rises from ~5 s^{-1} at the inception of microscale wave breaking to ~22 s^{-1} at $U_{10} = 8.9$ m s^{-1}, with localized maximum values reaching well above 100 s^{-1} at the higher wind speeds. These values are significantly higher than results from recent overhead-PIV studies (Xu, Khoo *et al*. 2006; Turney, Smith *et al*. 2005) but are more believable in the context of recent side-view-PIV

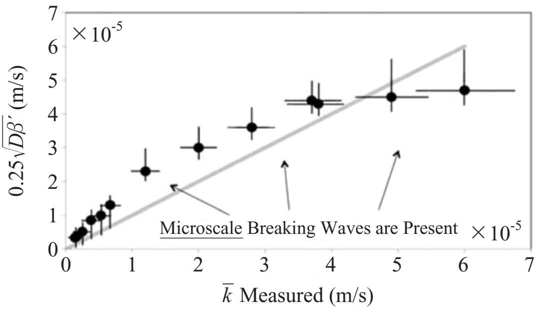

Figure 6 A comparison of the McCready *et al.* (1986) surface divergence theory against direct measurements of the interfacial transfer rate, for wind sheared flows.

studies (Pierson and Banner 2003; Siddiqui and Loewen *et al.* 2004; Siddiqui and Loewen 2007) and infrared studies by (Zappa and Asher 2004). A viewing of the raw videos of our flow tracers gives us confidence in the higher surface divergence values found in our present investigation.

Figure 6 shows the comparison between the McCready *et al.* (1986) surface divergence prediction $\bar{k}=C\sqrt{D\beta'}$, as calculated from our measurements of β', and our direct measurements of $\bar{k}$ in windy conditions. Disagreement is seen between the theory and measurements. The theoretical predictions rise quickly at the inception of microscale breaking but then levels off as the wind speed gets larger. In the microscale breaking range of wind speeds, the relationship between $\bar{k}$ and $\sqrt{\beta'}$ is non-linear. Error analysis of our measurements was carefully investigated, and are reported in Figure 6. We conclude that the disagreement between the surface divergence theory and our measurements could not be explained by measurement error. See Turney *et al.* (2009a) for full details.

To understand the disagreement between theory and experiment, we explored our instantaneous measurements of surface divergence. Figure 7 shows typical images of surface divergence on wind waves as wind speed increases. At wind speeds high enough to cause microscale breaking we observed a large fraction of the surface divergence related to parasitic capillary waves. These capillary waves create intense surface divergence patterns shaped like crescents on the front side of microscale breaking waves, as seen in Figure 7.

The capillary waves show strong surface divergence, but are not effective in bringing bulk water into contact the interfacial water, or vice versa, because i) they move water up and down in an oscillatory manner that does not bring new water to the interface, and ii) they do not stay in one Lagrangian location long enough to cause a persistent upwelling or downwelling of water. A theoretical analysis of the

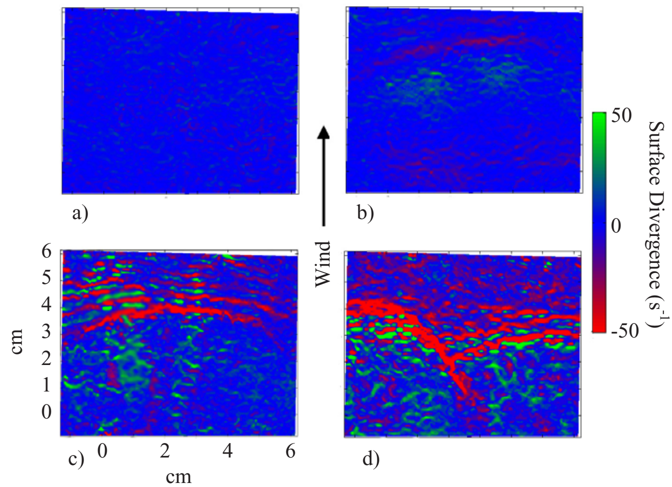

Figure 7 Images of our measurements of surface divergence for condtions a) $U_{10},=3.1$ m/s b) $U_{10},=4.1$ m/s, c) $U_{10},=7.1$ m/s, and d) $U_{10},=8.9$ m/s. A full color version of this plot exists on the digital version of this publication.

advection diffusion equation performed in Turney (2009a) gave the minimum length of time that a near surface motions must persist in one location to affect the gas transfer rate. A simplified version of this analysis finds that $\beta\tau > 1$ is the criteria for an interfacial water motion with divergence strength β and lifetime τ to affect interfacial gas transfer rate. Our 3D-IPIV measurements allowed Lagrangian tracking of parcels of surface water, and also allowed simultaneous recording of the surface divergence strength and wave morphology. A typical such time series is shown in Figure 8, for which a microscale breaking wave passes over the location for the Lagrangian analysis. On the front side of the wave, early in the time series, capillary waves create fast oscillations in surface divergence. On the backside of the wave a more persistent upwelling is observed which is not associated with a capillary wave, but rather, it is associated with turbulence generated by the passing breaking wave. As seen in the figure, the Lagrangian lifetime of the capillary oscillations do not satisfy $\beta\tau > 1$. However, the upwelling on the backside of the wave, which is not associated with capillary waves, does meet the requirement. The capillary waves were consistently found to be too short lived to meet the $\beta\tau > 1$ criteria.

We further investigated the matter by viewing our high-speed video of flow tracers backwards and manually following individual flow tracers until they disappeared into the bulk water. The length of time since the surface was renewed was thereby measured, i.e., the “age” of a parcel of surface water was measured.

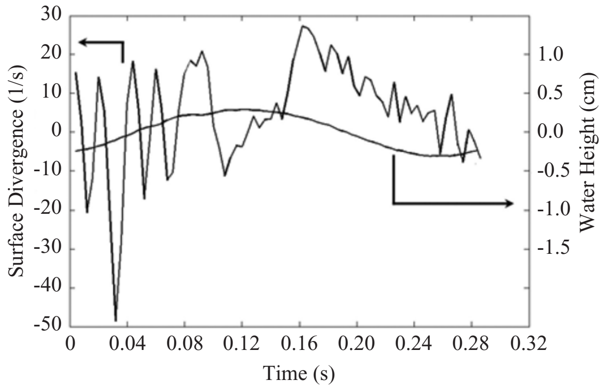

Figure 8 A Lagrangian time series of surface divergence following a surface parcel of water as a microscale breaking wave passes. The wind conditions were $U_{10}=6.0$ m/s.

Table 3 Statistics of our surface water "age" measurements.

Id	Mean Surface Age (s)	Capillary Wave Upwelling (%)	Laminar Wave Upwelling (%)	Turbulent Wave Upwelling (%)	Weak Upwelling (%)	Streamwise Streak (%)
W9	0.64	8	59	13	8	13
W11	0.53	5	46	28	5	15
W13	0.30	5	26	51	5	13

For each "age" measurement, we also recorded the type of event that generated the parcel of surface water, i.e., a capillary wave upwelling, a laminar wave upwelling, a turbulent wave upwelling, a weak upwelling, or a streamwise vortex. For wind conditions W9, W11, and W13, we made forty of these measurements, scattered at random locations in our video data. Table 3 presents the results of this investigation.

The results, given in Table 3, show that capillary waves cause surface renewal in less than 10% of the cases. Usually the surface renewal is on the backside of the wave. The results also show that turbulence plays a more important role at higher wind speeds, i.e., the microscale breaking waves at lower wind speeds bring less turbulence into play than those at higher wind speeds. These findings support those from (Siddiqui *et al*. 2004; Siddiqui and Loewen 2007) and (Zappa, *et al*. 2004) who found that the area covered by turbulent wakes increased dramatically as wind speeds rose through the microscale breaking range.

To better explain our measurements, we generated a new mechanistic model of air-water gas transfer that is a unification of the surface renewal concept and the

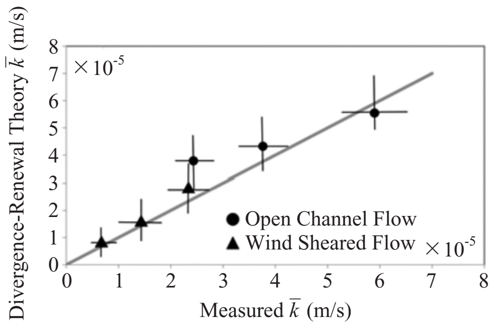

Figure 9 Comparison of our new model of the air-water gas transfer coefficient $\bar{k}$ against direct measurements of $\bar{k}$. The solid line is the one-to-one agreement line. Lines extending from the data points give our measurement error.

surface divergence concept. The new model assumes that the most important motions are upwellings of strength β' separated in time from by an average renewal time of τ. The approach begins with the full advection-diffusion equation and takes the same route as Danckwerts (1951), but rather than assuming each renewal event to completely renew the interface with fresh water, we assume each renewal event to bring the surface water to equilibrium with surface divergence of strength β'. This generates the following prediction for the gas transfer coefficient

$$\bar{k}=\sqrt{\frac{D}{\tau}}e^{\frac{1}{2\beta'\tau}}erfc\left(\sqrt{\frac{1}{2\beta'\tau}}\right). \tag{2}$$

Our 3D-IPIV data give values for β' and our measurements in Table 3 give values for τ, therefore we are able to fully calculate equation (2) with the data of Table 3 and Figure 6. To extend the calculations into our open channel flow conditions we gathered measurements on the same manner as in Table 3 but for flow conditions R6, R9, and R12. Figure 9 shows predictions of $\bar{k}$ from equation (2) compared to our direct measurements of $\bar{k}$, for both wind sheared and open channel flows. Good agreement is found, which is exceptional considering that no corrective coefficient has been placed in front of the predictions.

4. Conclusions

The relationship between the near-surface motions and the gas transfer coefficient has been analyzed in the light of computational simulations and laboratory measurements. The surface divergence theories of McCready *et al.* (1986) and Banerjee (1990) agree with measurements in open channel flows, in the absence of wind shear. However, measurements in wind sheared flows find that the inception of capillary waves causes the relation between β' and $\bar{k}$ to be non-linear. The persistence of motions in a Lagrangian frame due to capillary waves is found to be too short to affect the interfacial gas transfer rate. It is shown that $\beta\tau > 1$ is required for motions to be effective in gas transfer which requires a combination of surface divergence and renewal time to be calculated. The region of wind waves trailing the crest is found to be the site of upwellings that persist long enough to cause transfer. In low wind speed microscale breaking this region contains large upwellings of a laminar nature, but at higher wind speed microscale breaking the region is filled with turbulent motions. To address these new findings, a combination of the surface renewal and surface divergence theories is developed and is found to agree with measurements of $\bar{k}$, which is particularly encouraging since it does not use any corrective coefficients to find agreement with empirical measurements.

Acknowledgements

We gratefully acknowledge financial support from the US National Science Foundation grant CTS-055333, and from the US Department of Energy grant DE-FG03-85ER13314. We also thank Ira Leifer, Brian Piorek, Channimalikarjun Mathpati, Angelika Anderer, and Michael Zavrel for valuable work towards gathering these results.

References

Banerjee, S. (1990), Turbulence Structure and Transport Mechanisms at Interfaces, *Ninth International Heat Transfer Conference, Keynote Lectures*. Hemisphere Press, 395-418.

Banerjee, S., D. S. Scott, and E. Rhodes (1968), Mass Transfer to Falling Wavy Liquid Films in Turbulent Flow, *Industrial & Engineering Chemistry Fundamentals*, 7(1): 22-27.

Danckwerts, P. V. (1951), Significance of Liquid-Film Coefficients in Gas Absorption, *Industrial and Engineering Chemistry*, 43(6): 1460-1467.

De Angelis, V., P. Lombardi, P. Andreussi, S. Banerjee (1998), Microphysics of Scalar Transfer at Air-Water Interfaces, *Proceedings of the IMA Conference: Wind-over-Wave Couplings, Perspectives and Prospects.* (ed. Sajjadi, Hunt and Thomas), Oxford Press, 257-271.

Fortescue, G. and J. R. A. Pearson (1967), On Gas Absorption into a Turbulent Liquid. *Chemical Engineering Science*, 22(9): 1163-1167.

Fulgosi, M., D. Lakehal, S. Banerjee, S., and De Angelis, V. (2003), Direct Numerical Simulation of Turbulence in a Sheared Air-water Flow with a Deformable Interface, *Journal of Fluid Mechanics,* 482, 319-345.

Higbie, R. (1935), The Rate of Absorption of a Pure Gas into a Still Liquid During Short Periods of Exposure. *Transactions of the American Institute of Chemical Engineers,* 31, 365.

Hunt, J. C. R. and J. M. R. Graham (1978), Free-stream turbulence near plane boundaries, *J.*

Fluid Mech., 84, 209-235.

Hunt, J. C. R., S. Belcher, D. Stretch, S. Sajjadi and J. Clegg (2010), Turbulence and wave dynamics across gas-liquid interfaces, *The 6th international symposium on gas transfer at water surfaces*.

Komori, S., R. Nagaosa and Y. Murakami (1993), Turbulence structure and mass transfer across a sheared air-water interface in wind-driven turbulence, *J. Fluid Mech., 249*, 161-183.

Lam, K. and S. Banerjee, (1992), On the Conditions of Streak Formation in Bounded Flows, *Physic of Fluid*s, A4, 306-320

Lewis, W. K. and W. G. Whitman (1924), Principles of Gas Absorption. *Industrial & Engineering Chemistry*, 16: 1215.

Lombardi, P., V. DeAngelis and S. Banerjee (1996), Direct Numerical Simulation of Near-Interface Turbulence in Coupled Gas-Liquid Flow, *Physics of Fluids*, 8, 1643

McCready, M. J., E. Vassiliadou, *et al*. (1986), Computer-Simulation of Turbulent Mass-Transfer at a Mobile Interface. *AIChE Journal*, 32(7): 1108-1115.

Peirson, W. L. and M. L. Banner (2003), Aqueous Surface Layer Flows Induced by Microscale Breaking Wind Waves, *Journal of Fluid Mechanics*, 479: 1-38.

Siddiqui, M. H. K. and M. R. Loewen (2007), Characteristics of the Wind Drift Layer and Microscale Breaking Waves, *Journal of Fluid Mechanics*, 573: 417-456.

Siddiqui, M. H. K., M. R. Loewen, *et al*. (2004), Coherent Structures beneath Wind Waves and Their Influence on Air-Water Gas Transfer, *Journal of Geophysical Research-Oceans*, 109(C3).

Turney, D., W. C. Smith, and S. Banerjee. (2005), A Measure of near-Surface Fluid Motions That Predicts Air-Water Gas Transfer in a Wide Range of Conditions, *Geophysical Research Letters*, 32(4).

Turney, D. E. (2009a), Improved Understanding of Air-Water Transfer of Volatile Chemicals. *PhD Dissertation in the Donald Bren School of Environmental Science & Management,* University of California, Santa Barbara.

Turney, D. E., A. Anderer, and S. Banerjee. (2009b), A Method for Three-Dimensional Interfacial Particle Image Velocimetry (3D-IPIV) of an Air-Water Interface, *Measurement Science & Technology*, 20(4),

Xu, Z. F., B. C. Khoo (2006), Mass Transfer across the Turbulent Gas-Water Interface, *AIChE Journal*, 52(10): 3363-3374.

Zappa, C. J., W. E. Asher, *et al.* (2004), Microbreaking and the Enhancement of Air-Water Transfer Velocity, *Journal of Geophysical Research-Oceans*, 109(C8),